Electromagnetic analysis of COMPASS-U vacuum vessel during fast transients

V. V. Yanovskiy[a], N. Isernia[b], V. D. Pustovitov[c,d], F. Villone[b], D. Abate[e], P. Bettini[e], S. L. Chen[f], J. Havlicek[a], A. Herrmann[g], J. Hromadka[a], M. Hron[a], M. Imrisek[a], M. Komm[a], R. Paccagnella[e], R. Panek[a], G. Pautasso[g], S. Peruzzo[e], D. Sestak[a], M. Teschke[g], I. Zammuto[g] and the COMPASS team

[a]*Institute of Plasma Physics of the CAS, Prague, Czech Republic*
[b]*Consorzio CREATE, DIETI, Università degli Studi di Napoli Federico II, Italy*
[c]*National Research Centre Kurchatov Institute, Moscow, Russia*
[d]*National Research Nuclear University MEPhI, Moscow, Russia*
[e]*Consorzio RFX, Corso Stati Uniti 4, 35127 Padova, Italy*
[f]*Institute of Plasma Physics, Chinese Academy of Sciences, PO Box 1126, Hefei 230031, People's Republic of China*
[g]*Max-Planck-Institut für Plasmaphysik, EURATOM Association, D-85740 Garching, Germany*
[h]*Charles University, Faculty of Mathematics and Physics, Prague, Czech Republic*

The poloidal distribution of electromagnetic loads during fast transients in the vacuum vessel of COMPASS-U tokamak is calculated analytically. The analytical estimates are compared with CarMa0NL and ANSYS numerical simulations. The results show that the force-free condition for the plasma is necessary for the proper modelling of disruptions in the COMPASS-U tokamak.

Keywords: tokamak, COMPASS-U, vacuum vessel, disruption, electromagnetic loads

1. Introduction

This paper presents the analysis of disruptions in COMPASS-U tokamak [1], which is a medium-size high-magnetic-field device currently in the conceptual design phase. Due to the high plasma current (up to 2 MA) and strong magnetic field (up to 5 T), large electromagnetic forces on conducting structures surrounding plasma are expected during disruptions. To address this issue, first, the electromagnetic loads (EM) on the vacuum vessel (VV) are estimated analytically using a novel approach to the problem [2-4]. Then, these analytical estimates are compared with CarMa0NL [5,6] and ANSYS numerical simulations.

To guarantee the structural integrity of a tokamak and its components, during the design phase it is important to consider realistic distribution of the EM loads. Our analysis shows that the force-free condition for plasma must be applied for proper modelling of fast transients in COMPASS-U tokamak.

2. Analytical estimates

2.1 Results for plasma with force-free condition (A1)

To estimate the distribution of EM forces during disruptions, we approximate the 3D VV of COMPASS-U tokamak, shown in Fig. 1, by a circular tokamak with major radius $R_0 = 1m$ and minor radius $b_w = 0.5m$, as illustrated in Fig. 2. For COMPASS-U plasma of minor radius $b = 0.3m$, with internal inductance $l_i = 0.94$ and beta poloidal $\beta_J = 0.5$, the Shafranov shift Δ_{iw} calculated with formula (53) from [2] is 0.1 m, and the plasma major radius is $R = R_0 + \Delta_{iw} = 1.1m$.

Results in [2] are valid for the case when the vacuum vessel reacts on perturbations as an ideal conductor. First, we verify this assumption, the characteristic resistive wall time is $\tau_w \equiv \mu_0 b_w d_w / \eta \approx 5ms$, where $\mu_0 = 4\pi \times 10^{-7} H \cdot m^{-1}$ is the vacuum magnetic permeability, $d_w \approx 1cm$ is the wall thickness and $\eta = 1.26 \mu\Omega \cdot m$ is the electrical resistivity of Inconel 625. According to the scaling laws [7], for the COMPASS-U tokamak one can expect $\tau^*_{TQ} << \tau_w$ and $\tau^*_{CQ} << \tau_w$, where τ^*_{TQ} and τ^*_{CQ} are the times for the fastest thermal quench (TQ) and current quench (CQ), respectively. In these cases, we can treat the wall as ideal and use formula (69) from [2] for the poloidal distribution of the surface density of the normal magnetic force acting on the wall during disruption,

$$\mathbf{f}_w = \mathbf{n}_w \delta p_m = \mathbf{n}_w (\delta p_{m0} + \delta p_{m1} \cos u), \qquad (1)$$

where $\mathbf{n}_w$ is outwardly directed unit normal to the wall, $\delta p_m = p_m(t) - p_m(t_0)$ is the variation of the magnetic pressure at the inner side of the wall $p_m \equiv \mathbf{B}^2 / (2\mu_0)$, before t_0 and after t fast transient event,

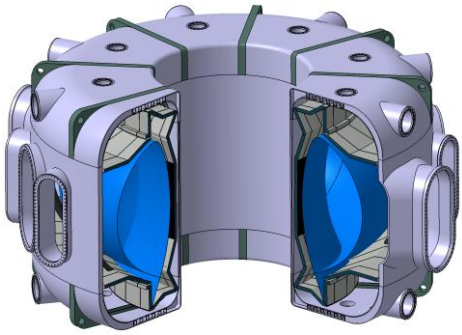

Fig. 1. Vacuum vessel of COMPASS-U tokamak

author's email: yanovskiy@ipp.cas.cz

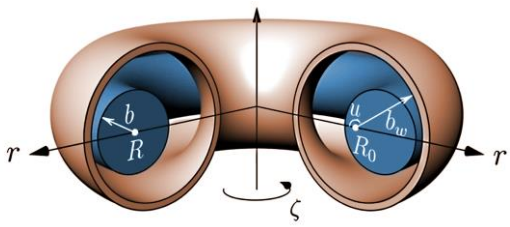

Fig. 2. Geometry of the problem, the cylindrical coordinates (r,ξ,z) related to the main axis of the system, R_0 and b_w are the wall major and minor radii, respectively; R and b are the similar plasma parameters.

u is the polar angle linked to geometrical center of the wall (in the poloidal cross-section), δp_{m0} and δp_{m1} are the variations of amplitudes of $m=0$ and $m=1$ poloidal harmonics, respectively:

$$\delta p_{m0} = \kappa^2 \delta \bar{p}, \tag{2}$$

$$\delta p_{m1} = -\varepsilon_w \kappa^2 \delta(B_J^2 l_w)/2\mu_0, \tag{3}$$

where $\kappa \equiv b/b_w$ and $\varepsilon_w \equiv b_w/R$, $\bar{p}$ is the mean plasma kinetic pressure, $B_J \equiv \mu_0 J/(2\pi b)$ is the averaged poloidal magnetic field at the plasma boundary, J is the net plasma current, $l_w \equiv l_i + 2\ln(b_w/b)$ and $l_i \equiv \bar{B}_p^2/B_J^2$ is the internal inductance per unit length of plasma column with B_p the poloidal magnetic field.

For COMPASS-U scenario with $\beta_J \equiv 2\mu_0 \bar{p}/B_J^2 = 0.5$ and $J = 2\,MA$ from (2) we find $\delta p_{m0} \approx -0.13\,MPa$, which means that large magnetic pressure on the wall develops already during TQ. For the same parameters and $l_i = 0.94$ from (3) it follows that the magnetic pressure on the wall during CQ is $\delta p_{m1} \approx 0.22\,MPa$. The integral radial TQ and CQ-related forces are

$$F_r^{TQ} = 0.5 S_w \varepsilon_w \delta p_{m0} \approx -0.7\,MN \text{ and} \tag{4}$$

$$F_r^{CQ} = -0.5 S_w \delta p_{m1} \approx -2.4\,MN, \tag{5}$$

respectively. Here $S_w \equiv (2\pi)^2 R b_w$ is the full lateral area of the wall. For comparison with numerical results, we consider only the CQ-related force, its poloidal distribution, for the above case, is shown in Fig. 3a.

2.2 Results for plasma represented by toroidal filaments (A2)

According to [2-4] for the wall and/or plasma represented by toroidal filaments the poloidal distribution of the EM force, is given by

$$\delta p_m^{\psi} = \delta p_{m0}^{\psi} + \delta p_{m1}^{\psi} \cos u = \\ = \kappa^2 \delta \left\{ B_J^2/(2\mu_0) \left[1 - 2\varepsilon_w (\beta_J + l_w/2 - 1) \cos u \right] \right\}. \tag{6}$$

For a CQ with $\delta J = 2\,MA$ and $\delta\beta_J = 0$, the amplitude of the $m=1$ harmonic in the above expression is negligible with respect to the fundamental one $\delta p_{m1}^{\psi}/\delta p_{m0}^{\psi} = 0.02$. Formula (1), derived for plasma satisfying Grad-Shafranov equation and a continuous wall, instead, predicts only $m=1$ harmonic for the same CQ. From formula (5) we find $\delta p_{m0}^{\psi} \approx -0.25\,MPa$ and $\delta p_{m1}^{\psi} \approx -0.005\,MPa$. The poloidal distribution of δp_m^{ψ} is shown in Fig. 3b. The corresponding integral radial force $F_r^{\psi} = [(l_w - 1)/l_w] F_r^{CQ} \approx 0.5 F_r^{CQ}$ differs in magnitude with respect to the case considered in Section 2.1. We notice that it can even change direction for $l_w < 1$.

3. Numerical results

In this section, first, we compare analytical predictions for the plasma satisfying force-free condition (Fig. 3a) with CarMa0NL results, presented in Figs. 4a and 5a. Then, the analytical estimates for the plasma represented by toroidal filaments and therefore not satisfying the Grad-Shafranov equation (Fig. 3b) are compared with ANSYS results, shown in Figs. 4b and 5b.

The initial equilibrium parameters used for the simulations are reported in Table. 1. The main difference with the setup for analytics is that the plasma column is shifted inwards and not outwards, accordingly, the plasma major radius is $R = 0.9\,m$ instead of $R = 1.1\,m$. In this way we can study the worst case scenario for the inner side of the vessel and, consequently, decide on its thickness.

The vertical magnetic field is produced by four poloidal field coils. Two upper coils are centered at $(r = 0.25, z = 0.75)$ and $(1.75, 0.75)$, with -3.76 MA and -0.86 MA current, respectively. Two lower coils are situated symmetrically with respect to the $z = 0$ plane.

3.1 CarMa0NL modelling

CarMa0NL [5,6] solves 2D nonlinear evolutionary equilibrium MHD equations, self-consistently coupled to eddy currents equations, describing 3D volumetric conductors. Despite the 2D nature of the problem under consideration, the choice of CarMa0NL is suggested by the need to include poloidal eddy currents generated in the conducting structures, a rare feature for a disruption study oriented MHD code. A plasma disruption is modelled by a very fast 2MA/0.01ms current quench. During such an abrupt electromagnetic event 1cm thick Inconel 625 vessel behaves as an ideal wall. Moreover, in 0.01ms timeframe the plasma does not change significantly its position and shape, this allows a comparison with above analytical predictions. The found poloidal distribution of EM force is presented in Fig. 4a, where both components, normal and tangential to the wall are kept. In contrast, in Fig. 5a only normal component is kept easing comparison with analytical estimates shown in Fig. 3a.

Amplitudes for the first five harmonics of magnetic pressure δp_m, and the total radial force, calculated with tangential component $F_{r,tot}$, and without taking it into account $F_{r,norm}$, are reported in Table 2. For this modelling the poloidal beta was adjusted to be as low as $\beta_J = 0.13$, to consider primarily CQ-related force and diminish the TQ-related component. However, according to (2) the variation of $\delta\beta_J = 0.13$ still provides a small contribution to the fundamental harmonic $\delta p_{m0} = -0.03\,MPa$, therefore, the numerical result $\delta p_{m0} = +0.02\,MPa$ may be an underestimate.

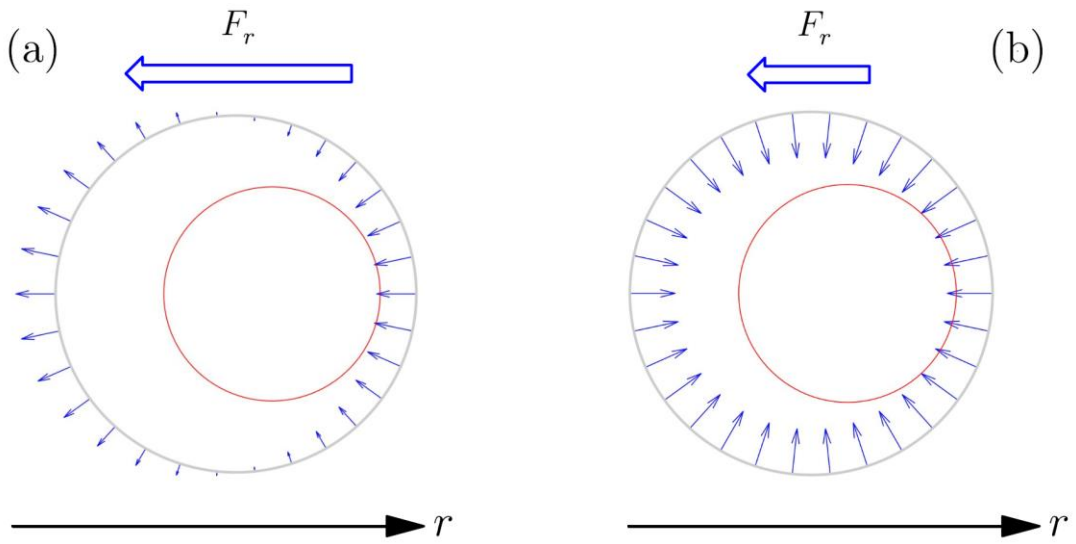

Fig. 3. Analytical results for the poloidal distribution of the CQ-related force, normal to the tokamak wall, for COMPASS-U parameters, with (a) and without (b) account of the poloidal current in the wall. The upper thick arrows show the integral radial forces.

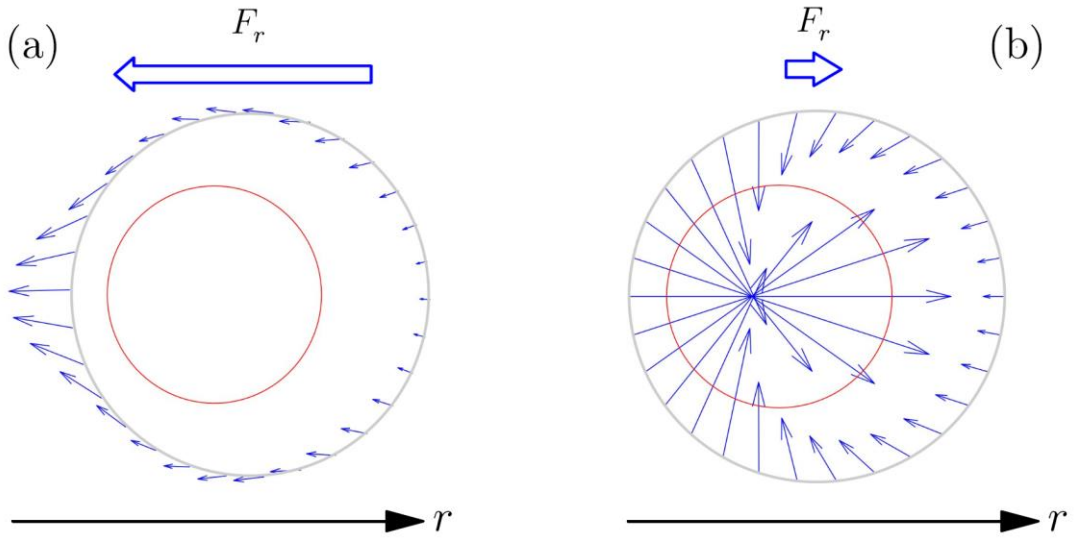

Fig. 4. Numerical results for the poloidal distribution of the CQ-related force on the tokamak wall obtained with CarMa0NL (a) and ANSYS (b) for COMPASS-U parameters. The upper thick arrows show the integral radial forces.

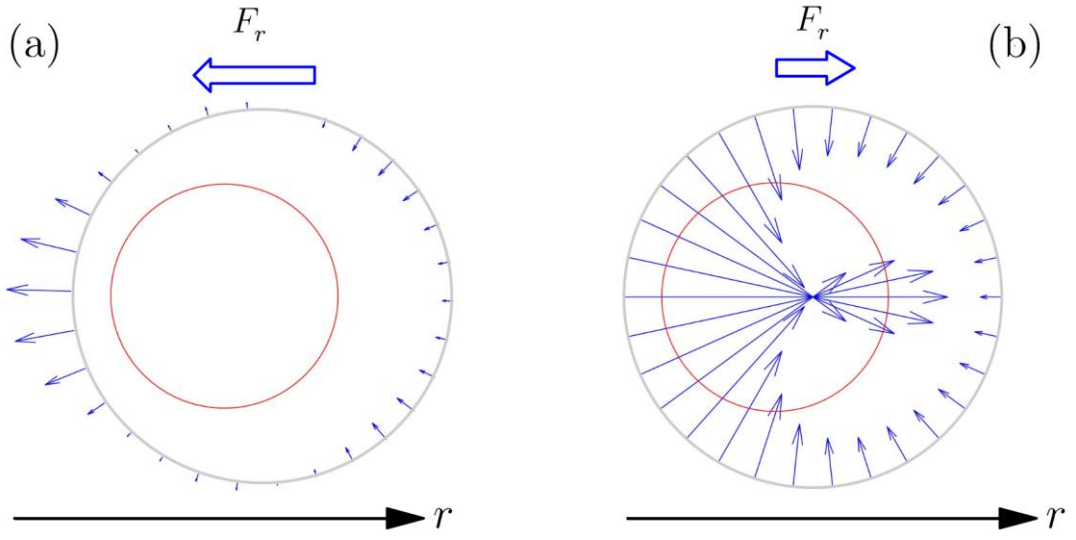

Fig. 5. Numerical results for the poloidal distribution of the CQ-related force, normal to the tokamak wall, obtained with CarMa0NL (a) and ANSYS (b) for COMPASS-U parameters. The upper thick arrows show the integral radial forces.

3.2 ANSYS modelling

The transient problem is solved in ANSYS Electronics with plasma represented by one fixed toroidal conductor with 2MA current that decreases to zero in 0.01ms. The current is distributed uniformly across a channel of minor radius $a = 0.24m$ and major radius $R = 0.9m$, with internal inductance $l_a = 0.5$. In this way at $b = 0.3m$, the internal inductance is the same as for other cases, $l_i = l_a + 2\ln(b/a) = 0.94$.

Results for δp_m, $F_{r,tot}$ and $F_{r,norm}$, at the end of CQ, are reported in Table 2. The poloidal distribution of the EM force and its normal component are shown in Figs. 4b and 5b, respectively.

Table 1. Main parameters for numerical simulations with CarMa0NL and ANSYS model, and for analytical calculations with (A1) and without (A2) force-free condition for plasma.

	A1	CarMa0NL	A2	ANSYS
$\delta J, MA$	2	2	2	2
$\delta\beta_J$	0	0.13	0	NA
l_i	0.94	0.94	0.94	0.94 (0.5)
R, m	1.1	0.9	1.1	0.9
b, m	0.3	0.3	0.3	0.3(0.24)

Table 2. Analytical results for plasma with (A1) and without (A2) force-free condition, and numerical results obtained with CarMa0NL for plasma satisfying Grad-Shafranov equation and ANSYS for plasma represented by a toroidal filament.

	A1	CarMa0NL	A2	ANSYS
$F_{r,tot}, MN$	NA	-2.7	NA	0.4
$F_{r,norm}, MN$	-2.4	-1.2	-1.2	0.8
$\delta p_{m0}, MPa$	0.00	0.02	-0.25	-0.60
$\delta p_{m1}, MPa$	0.22	0.14	-0.005	-0.69
$\delta p_{m2}, MPa$	0	0.05	0	-0.32
$\delta p_{m3}, MPa$	0	0.03	0	-0.11
$\delta p_{m4}, MPa$	0	0.06	0	0

4. Discussion and conclusions

Comparing Figures 3a and 3b with 5a and 5b, respectively, one can see good qualitative agreement between analytical and numerical results. The quantitative difference may be caused by two factors, first, results in [2-4] are derived for a circular vessel with high aspect ratio, we instead considered $R_0/b_w = 2$. Second, the initial equilibrium is different, as the plasma column is shifted inwards for the numerical analysis and outwards for the analytical one.

The difference between CarMa0NL and ANSYS results is drastic. For example, the magnetic pressure at the inner side of the torus calculated with ANSYS model $\delta p_m = -1.72 MPa$ is almost 6 times higher with respect to the CarMa0NL value $\delta p_m = 0.30 MPa$, which also differs in sign. At the same time ANSYS model underestimates in 7 times the absolute value of the total radial force and predicts it in the opposite direction with respect to the CarMa0NL result, $F_{r,tot}^{CQ} = 0.4 MN$ against $F_{r,tot}^{CQ} = -2.7 MN$. This discrepancy is due to the absence of poloidal eddy currents in the ANSYS model, since the plasma is represented by a toroidal filament and only toroidal eddies are induced in the vessel.

The EM force related to poloidal eddies is stronger at this inner side of the torus for the following reason. For the circular VV with $(R_0 + b_w)/(R_0 - b_w) = 3$, the length of the internal circumference of the torus is 3 times smaller with respect to the external one, this makes the density of poloidal currents 3 times larger at $r = R_0 - b_w$. Moreover, as the toroidal magnetic field decreases as $1/r$, it is 3 times larger at the internal side. This results in 9-fold difference for the EM force related to poloidal eddies at inner and outer parts of the vessel. It is effect is beneficial in the sense that it compensates the EM force related to toroidal currents.

The analytical theory [2-4], shows that the representation of the plasma by toroidal filaments leads to a completely different poloidal distribution of the EM force, with respect to models where plasma satisfies Grad-Shafranov equation. Our numerical study demonstrates that for the parameters of COMPASS-U tokamak this difference is even larger than predicted by analytics. The ANSYS modelling can provide an order of magnitude lower value for the total radial force and at the same time overestimate significantly the magnetic pressure at the inner side of the vessel.

Acknowledgments

This work has been carried out within the framework of the project COMPASS-U: Tokamak for cutting-edge fusion research No. CZ.02.1.01/0.0/0.0/16_019/0000768 and co-funded from European structural and investment funds.

References

[1] R. Panek et al., Fusion Eng. Des. 123 (2017) 11.
[2] V.D. Pustovitov and D.I. Kiramov, Plasma Phys. Control. Fusion 60 (2018) 045011.
[3] V.D. Pustovitov, Filament representation of the plasma in the tokamak disruption studies, P2.1036, in: Proceedings of 45th EPS Conference on Plasma Physics, Prague, Czech Republic, 2018.
[4] V.D. Pustovitov, Phys. Plasmas 25 (2018) 062510.
[5] F. Villone et al., Plasma Phys. Control. Fusion 55 (2013) 095008.
[6] F. Villone et al., Parametric dependence analysis of disruption forces in tokamaks, P4.1047, in: Proceedings of 45th EPS Conference on Plasma Physics, Prague, Czech Republic, 2018.
[7] ITER Physics Expert Group on Disruptions, Plasma Control and MHD, Nucl. Fusion 39 (1999) 2251.